WWW.IJRPR.COM

International Journal of Research Publication and Reviews

Journal homepage: www.ijrpr.com ISSN 2582-7421

Effect of Chemical Reaction on Unsteady MHD Flow of Jeffery Fluid in a Porous Enclosure Bounded by a Vertical Oscillating Cylindrical Surface

A. K. Shukla[1,*], Aneesh Jayswal[2], Mohammad Suleman Quraishi[3]

[1,2,] Department of Mathematics, RSKD PG College, Jaunpur, U.P., India
[3]Department of Applied Sciences, Jahangirabad Institute of Technology, Barabanki, U.P., India

A B S T R A C T

In this study, using the motion of a vertical oscillating cylinder in an unsteady MHD Jeffery fluid flow with heat radiation through a porous media and chemical reaction, we explored the effects of various flow parameters. A set of nonlinear partial differential equations govern the problem's mathematical model. Using the Crank Nicolson finite difference approach, the partial differential equations that control flow have been quantitatively solved. Results have been disclosed by the cylinder's radius and distance from the wall (cylinder). Tables are used to show the properties of skin friction, the Nusselt number, and the Sherwood number, while graphs are used to show the characteristics of velocity, temperature, and concentration.

Keywords: Crank Nicolson Method, Jeffery Fluid, Magnetohydrodynamics (MHD) Flow, Radiation.

I. 1. Introduction

For each experiment in the prior-year literature reviews, only the Newtonian fluid model was used. Very little research has been done to examine how non-Newtonian fluids flow in porous-walled channels and tubes, despite the fact that the majority of industrial and biological fluids are non-Newtonian and the classical Newton's law of viscosity fails to describe the complex rheological properties of non-Newtonian fluids. One non-Newtonian fluid model that has drawn attention from researchers is the Jeffrey fluid model, which is thought to be the best model for physiological fluids. The unsteady MHD Jeffery flow on a vertical porous plate with first order chemical reaction is of interest to many mathematicians. In recent years, it has become more crucial than ever to examine how mass transfer affects both Newtonian and non-Newtonian fluids. Heat transmission through radiation is used in many different industries, including semiconductor wafer manufacturing, the production of transient crystals, energy transfer in furnaces, and solar energy. Engines and combustion chambers are designed to run at greater temperatures to boost thermal efficiency. Flow happens in solid mechanics because of the wide range of natural convection MHD applications used in the chemical industry, including drying, food processing, oil extraction, and other processes. This is the motivating factor for many researchers to pursue this field of study. Moreover, astrophysical flows as well as the heating and cooling of thermal chambers typically employ radiative-convective flow. The fluid dynamics theory of mass transfer is applied in the burning oil pool, leaching by spray, and drying. Several scientists and engineers have studied the impacts of Soret and Dufour on flow issues because of their applications in such fields, such as isotope separation.

The numerical result of nonlinear radiation for nanofluid heat transport across a vertical plate was examined by Sandeep and Babu [1]. Unsteady nanofluid flow phenomena in the presence of chemicals of a higher order were studied by Rushi et al. [2]. A power-law fluid's MHD boundary layer slip flow and heat transfer over a flat plate were the focus of Mastroberardino et al. [3] research. The change Soret-Dufour on MHD flow of a viscoelastic fluid over a semi-infinite vertical plate is examined by Idowu and Falodun [4]. The combined effects of Soret and Dufour on the MHD flow of a power-law fluid across a flat plate in a slip flow regime were investigated by Saritha et al. [5]. The effects of second-order chemical reaction on MHD free convection dissipative fluid flow past an inclined porous surface by way of Heat Generation were examined by Malik and Rahman [6]. In the flow of a viscous fluid by a curved stretching surface, Imtiaz et al. [7] observed the effects of Soret and Dufour. In a porous media, MHD mixed convection flow towards a vertical plate was investigated by Anuradha and Harianand [8]. The precise solution of Heat and mass transport in MHD Poiseuille flow with porous walls was investigated by Ahmed [9]. In the presence of a heat source and chemical reaction, Das and Dorjee [10] examined the MHD flow with Soret and Dufour effects. In the presence of Newtonian heating, a nonlinear radially stretched sheet causes a Jeffrey liquid to flow in MHD, according to T. Hayat et al. [11]. S. Sreenadh and M. Eswara Rao [12] describes the MHD Boundary Layer Flow of Jeffrey Fluid over a stretching/shrinking sheet through a porous medium. Simultaneous impacts of melting heat and internal heat generating instagnation point flow of Jeffrey fluid approaching a nonlinear stretching surface with varying thickness, T. Hayat et al. [13]. Three-dimensional Couette flow of a Jeffrey fluid along periodic injection/suction, M.A. Rana et al. [14]. M.A. Imran [15], uniform heat flux and MHD fractional Jeffrey's fluid flow with thermodiffusion, thermal radiation effects, and first order chemical reactions. Radiative Flow of Jeffrey Fluid Across a Convectively Heated Stretching Cylinder, T. Hayat et al. [16]. Radiative flow of MHD

Jeffrey fluid past a stretching sheet with surface slip and melting heat transfer, K. Das et al. [17]. M. Ali Abbas and M.M. Bhatti Simultaneous effects of slip and MHD on the Jeffrey fluid model's peristaltic blood flow through a porous medium are discussed in [18]. Peristaltic pumping of a power-Law fluid in contact with a Jeffrey fluid in an inclined channel with porous walls, S. Sreenadh et al. [19]. Magneto hydrodynamic peristalsis of variable viscosity Jeffrey liquid with heat and mass transfer, S. Farooq et al. [20]. Unsteady MHD Mixed Convection of Jeffrey Fluid Past an Inclined Permeable Moving Plate in the Presence of Thermophoresis Heat Production and Chemical Reaction, K. Venkateswara et al. [21]. Multivariate Jeffrey Fluid Flow through a Vertical Plate via Porous Media, D. Dastagiri Babu et al. [22].

The aim of the present work is to analyze the effect of first-order chemical reaction on unsteady MHD Jeffery flow of viscous incompressible fluid through a vertical oscillating cylinder immersed in a porous medium. The results of variation in different parameters on velocity, heat transfer, and mass transfer as well as in physical quantities like skin friction, Nusselt number, and Sherwood number are received by solving the governing equations of the flow field with considering changes with appropriate parameters using Crank-Nicolson implicit finite difference method.

II. 2. Formulation of the problem

The flow of a viscous, incompressible electrically conducting fluid through an infinite, impulsively/oscillatorily started vertical cylindrical surface with customizable temperature and mass distribution, as well as chemical reaction and radiation effect, has been considered in the context of unsteady MHD Jeffery flow. The cylinder is upright and oscillating in a porous medium. The y-axis is seen as perpendicular to the cylinder and the x-axis as parallel to it. Also, it is first believed that the radiation heat flux in the x-direction is much smaller than that in the y-direction. The temperature and concentration of the fluid and the cylinder are identical. The cylinder's surface temperature and concentration decline exponentially over time when it is moved impulsively in the x direction against the gravitational field at time t. The flow variables are just functions of y and t since the x-direction is infinite. The governing partial differential equations for this unstable Jeffery MHD flow field problem are provided by the mathematical model using the standard Boussinesq's approximation:

1) 2.1 Continuity equation:

$$\frac{\partial v}{\partial y} = 0 \Rightarrow v = 0 \tag{1}$$

2.1 Momentum equation:

$$\frac{\partial u}{\partial t} = \left(\frac{\nu}{1+\lambda}\right)\left(\frac{\partial^2 u}{\partial r^2} + \frac{1}{r}\frac{\partial u}{\partial r}\right) + g\beta_T(T - T_\infty) + g\beta_C(C - C_\infty) - \frac{\sigma {B_0}^2 u}{\rho} - \frac{\mu u}{\rho K} \tag{2}$$

2) 2.2 Energy equation:

$$\rho C_p\left(\frac{\partial T}{\partial t}\right) = k\left(\frac{\partial^2 T}{\partial r^2} + \frac{1}{r}\frac{\partial T}{\partial r}\right) - \frac{\partial q_r}{\partial r} + a_T(T - T_\infty) + a_C(C - C_\infty) \tag{3}$$

$$\frac{\partial C}{\partial t} = D_C\left(\frac{\partial^2 C}{\partial r^2} + \frac{1}{r}\frac{\partial C}{\partial r}\right) - k_r(\bar{C} - \bar{C}_\infty) \tag{4}$$

$\bar{C}$ concentration $\bar{T}$ temperature $\bar{T}_\infty$temperature of free stream, $\bar{C}_\infty$concentration of free stream, λ is Jeffery fluid parameter, in Equation 4, $k_r(\overline{C} - \overline{C_\infty})$ has been introduced for first order chemical reaction, k_r is chemical reaction constant β_c is coefficient of volume expansion for mass transfer , β_T is volumetric coefficient of thermal expansion, T_m mean fluid temperature, q_r radiative heat along y ∗ -axis, ν is kinematic viscosity, $\bar{K}$is coefficient of permeability of porous medium, D_c is molecular diffusivity, k is thermal conductivity of fluid, C_p denotes specific heat at constant pressure, μ is for viscosity, ρ fluid density, σ electrical conductivity, g is acceleration due to gravity.

The following are taken to be the model's boundary conditions:

$$\left.\begin{array}{ll} t = 0\,; & u(r,0) = 0, T(r,0) = \bar{T}_\infty, C(r,0) = C_\infty \forall r \\ t > 0\,; & u = u_0 Cos\omega t, T = T_\infty + (T_w - T_\infty)e^{-\alpha t}, \bar{C} = \bar{C}_\infty + (\bar{C}_w - \bar{C}_\infty)e^{-\alpha t} atr = R \\ & u \to 0, T \to T_\infty, C \to C_\infty asr \to \infty \end{array}\right\} \tag{5}$$

Where $\alpha = \frac{{v_0}^2}{\nu}$

Roseland explained the term radiative heat flux approximately as

$$q_r = -\frac{4\sigma_{st}}{3a_m}\frac{\partial T^4}{\partial r} \tag{6}$$

Here Stefan Boltzmann constant and absorption coefficient are $\sigma_{st}$and $a_m$respectively.

In this case temperature differences are very-very small within flow, such that $\bar{T}^4$ can be expressed linearly with temperature. It is realized by expanding in a Taylor series about T_∞' and neglecting higher order terms, so

$$T^4 \cong 4{T_\infty}^3 T - 3{T_\infty}^4 \tag{7}$$

With the help of equations (6) and (7), we write the equation (3) in this way

$$\rho C_p\left(\frac{\partial T}{\partial t}\right) = k\left(\frac{\partial^2 T}{\partial r^2} + \frac{1}{r}\frac{\partial T}{\partial r}\right) + \frac{16{T_\infty}^3\sigma_{st}}{3a_m}\frac{\partial^2 T}{\partial r^2} + a_T(T - T_\infty) + a_C(C - C_\infty) \tag{8}$$

Let us introduce similarity variables and the following dimensionless quantities as

$$\left.\begin{aligned}
&\xi = \frac{u}{u_0}, \tau = \frac{t{u_0}^2}{\nu}, \eta = \frac{r}{R}, \ \theta = \frac{T-T_\infty}{T_w-T_\infty}, \psi = \frac{C-C_\infty}{C_w-C_\infty}, \\
&G_c = \frac{\nu\, g\beta_c (C_w-C_\infty)}{{u_0}^3}, G_r = \frac{\nu\, g\beta (T_w-T_\infty)}{{u_0}^3}, K_p = \frac{{u_0}^2}{\nu^2} K, \\
&S_c = \frac{\nu}{D}, \ P_r = \frac{\mu C_p}{k}, \quad R_e = \frac{{u_0}^2 R^2}{\nu^2}, N = \frac{4\sigma_{st}\,\overline{T}_\infty^{\,3}}{a_m\, k}, a = \frac{{\nu_0}^2}{\nu}, \\
&M = \frac{\sigma {B_0}^2 \nu}{{u_0}^2}, A = \frac{{u_0}^2}{\nu}, B = \frac{a_c \nu (C_w-C_\infty)}{\rho C_p {u_0}^2 (T_w-T_\infty)}, K_r = \frac{k_r\, \nu}{{u_0}^2}
\end{aligned}\right\} \quad (9)$$

Using substitutions of Equation (9), we get non-dimensional form of partial differential Equations (2), (8) and (4) respectively

$$\frac{\partial \xi}{\partial \tau} = \left(\frac{1}{1+\lambda}\right)\frac{1}{{R_e}^2}\left(\frac{\partial^2 \xi}{\partial \eta^2} + \frac{1}{\eta}\frac{\partial \xi}{\partial \eta}\right) + G_r\theta + G_c\psi - \left(M + \frac{1}{K_p}\right)\xi \quad (10)$$

$$\frac{\partial \theta}{\partial \tau} = \frac{1}{P_r {R_e}^2}\left(\frac{\partial^2 \theta}{\partial \eta^2} + \frac{1}{\eta}\frac{\partial \theta}{\partial \eta}\right) + N\frac{\partial^2 \theta}{\partial \eta^2} + A\theta + B\psi \quad (11)$$

The constant A and B here are often very small and can be omitted in practice. So equation(11) becomes

$$\frac{\partial \theta}{\partial \tau} = \frac{1}{P_r {R_e}^2}\left(\frac{\partial^2 \theta}{\partial \eta^2} + \frac{1}{\eta}\frac{\partial \theta}{\partial \eta}\right) + N\frac{\partial^2 \theta}{\partial \eta^2} \quad (12)$$

$$\frac{\partial \psi}{\partial \tau} = \frac{1}{S_c {R_e}^2}\left(\frac{\partial^2 \psi}{\partial \eta^2} + \frac{1}{\eta}\frac{\partial \psi}{\partial \eta}\right) - K_r\psi \quad (13)$$

The boundary conditions for this model are assumed as:

$$\left.\begin{aligned}
&\tau = 0; \quad \xi = 0, \theta = 0, \psi = 0 \forall \eta \\
&\tau > 0; \quad \xi = Cos\gamma\tau, \theta = e^{-\tau}, \psi = e^{-\tau} at \eta = 1 \\
&\qquad \xi \to 0, \theta \to 0, \psi \to 0 \eta \to \infty
\end{aligned}\right\} \quad (14)$$

The degree of practical attention include the Skin friction coefficients Γ, local Nusselt Nu, and local Sherwood Sh numbers are known as follows:

$$\Gamma = \left(\frac{\partial u}{\partial y}\right)_{y=0}, \qquad N_u = -\left(\frac{\partial \theta}{\partial y}\right)_{y=0}, \qquad Sh = -\left(\frac{\partial C}{\partial y}\right)_{y=0} \quad (15)$$

III. 3. Mathematical Model for Solution

Analytical solution of system of partial differential Equations 10, 12 and 13 with boundary conditions given by Equation 14 is not possible. So, these equations, we have used to solve by Crank-Nicolson implicit finite difference method. The Crank-Nicolson finite difference implicit method is a second order method in time ($o(\Delta t^2)$) and space, hence no restriction on space and time steps, that is, the method is unconditionally stable. The computation is executed for $\Delta y = 0.1$, $\Delta t = 0.002$ and procedure is repeated till y = 4. Equations 10, 12 and 13 are expressed as

$$\frac{\xi_{i,j+1}-\xi_{i,j}}{\Delta\tau} = \left(\frac{1}{1+\lambda}\right)\left(\frac{1}{{R_e}^2}\right)\left(\frac{\xi_{i-1,j} - 2\xi_{i,j} + \xi_{i+1,j} + \xi_{i-1,j+1} - 2\xi_{i,j+1} + \xi_{i+1,j+1}}{2(\Delta\eta)^2} + \frac{1}{\Delta\eta}\frac{\xi_{i+1,j}-\xi_{i,j}}{\Delta\eta}\right)$$
$$+G_r\left(\frac{\theta_{i,j+1}+\theta_{i,j}}{2}\right) + G_c\left(\frac{\psi_{i,j+1}+\psi_{i,j}}{2}\right) - \left(M+\frac{1}{K_p}\right)\left(\frac{\xi_{i,j+1}+\xi_{i,j}}{2}\right) \quad (16)$$

$$\frac{\theta_{i,j+1}-\theta_{i,j}}{\Delta\tau} = \left(\frac{1}{P_r {R_e}^2} + N\right)\left(\frac{\theta_{i-1,j} - 2\theta_{i,j} + \theta_{i+1,j} + \theta_{i-1,j+1} - 2\theta_{i,j+1} + \theta_{i+1,j+1}}{2(\Delta\eta)^2}\right) + \left(\frac{1}{P_r {R_e}^2}\right)\frac{\theta_{i+1,j}-\theta_{i,j}}{\Delta\eta} \quad (17)$$

$$\frac{\psi_{i,j+1}-\psi_{i,j}}{\Delta\tau} = \frac{1}{{R_e}^2 S_c}\left(\begin{array}{c}\frac{\psi_{i-1,j} - 2\psi_{i,j} + \psi_{i+1,j} + \psi_{i-1,j+1} - 2\psi_{i,j+1} + \psi_{i+1,j+1}}{2(\Delta\eta)^2} \\ + \frac{1}{\Delta\eta}\frac{\psi_{i+1,j}-\psi_{i,j}}{\Delta\eta}\end{array}\right) - K_r\left(\frac{\psi_{i,j+1}+\psi_{i,j}}{2}\right) \quad (18)$$

Initial and boundary conditions are also rewritten as:

$$\xi_{i,0} = 0, \theta_{i,0} = 0, \psi_{i,0} = 0 \forall i$$
$$\xi_{0,j} = Cos\omega t, \theta_{0,j} = e^{-j\Delta t}, \psi_{0,j} = e^{-j\Delta t} \forall j$$
$$\xi_{l,j} \to 0, \theta_{l,j} \to 0, \psi_{l,j} \to 0 \quad (19)$$

Where index i represents to η and j represents to time τ, $\Delta\tau = \tau_{j+1} - \tau_j$ and $\Delta\eta = \eta_{j+1} - \eta_j$. Getting the values of ξ, θ and ψ at time τ, we may compute the values at time τ+Δτ as following method: we substitute i = 1, 2, ..., l−1 , where l correspond to ∞ ,equations 17 & 18 give tridiagonal system of equations with boundary conditions in equation 19, are solved employing Thomas algorithm as discussed in Carnahan et al.[23], we find values of θ and ψ for all values of η at τ + Δτ. Equation 16 is solved by same to substitute these values of θ and ψ, we get solution for ξ till desired time τ.

IV. 4. Investigations on Results

The goal of the current project is to assess the boundary layer unsteady MHD Jeffery flow on a cylindrical surface that is oscillating vertically. The numerical findings of the velocity profile, temperature profile, and concentration profile have been described with the use of graphs in order to see a physical view of the work, while skin friction coefficients, Nusselt number, and Sherwood number are presented using tables. The following values are used for investigation Gr = 7, Gc = 8, K= 3, N = 5, M = 4, Pr = 0.7, Sc= 3, λ = 1.5, ω =$\pi/4$. Figures 5 and 11 show that as parameter N is increased, temperature and velocity both rise. This is a valid observation because the rise in radiation indicates the movement of heat energy. Reynolds number has a significant impact on velocity and concentration distribution, as shown in Figures 3 and 15. Analysis shows that as Re increases, velocity and concentration fall. Figures 2 and 14 show how the Schmidt number Sc varies as velocity and concentration fall off as Sc increases. In figure 6, velocity reduces as magnetic parameter M is increased, along with a reduction in the momentum boundary layer. Figure 4 illustrates how velocity decreases as oscillation parameter ω is increased. Figures 1, 10, and 13 show that as time goes on, velocity, temperature, and concentration all raise. Figures 7 and 12 depict the temperature and velocity variations, which rise with increasing Prandtl number. Figure 8 shows the variational behaviour of the Jeffery fluid parameter as the Jeffery fluid parameter increases velocity increases. The effect of chemical reaction parameter Kr has been shown through Figures 9 and 16, when Kr increases then velocity and concentration decrease.

It is observed from **Table. I** that on increasing Schmidt number Sc, Reynolds's number Re, Magnetic parameter M, parameter N, Jeffery fluid parameter λ and chemical reaction parameter Kr effect skin friction coefficient Γ decreases while it increases with the increase in Prandtl number Pr, Oscillation parameter ω and time t. On increasing parameter N skin friction coefficient Γ increases and decreases simultaneously while it only decreases with the increase in Reynolds's number Re, Prandtl number Pr and time t. Sherwood number only increases only for Reynolds's number Re, Schmidt number Sc, time t and chemical reaction parameter Kr and remains same with the effect of other parameters.

V. 5. Conclusions

Effects of unsteady MHD flow past a vertical oscillating cylindrical surface in a porous medium have been analyzed. This investigation the following conclusions or outputs have come:

a) The flow velocity and temperature profile hike sharply over time.

b) It's interesting to note that when the Reynolds number R_e increases, velocity and concentration profiles decrease.

c) Schmidt number greatly influences the concentration profile in the concentration boundary layer.

d) Increase values of parameter Kr shows great influence of decrement on concentration profile and somewhat on velocity profile.

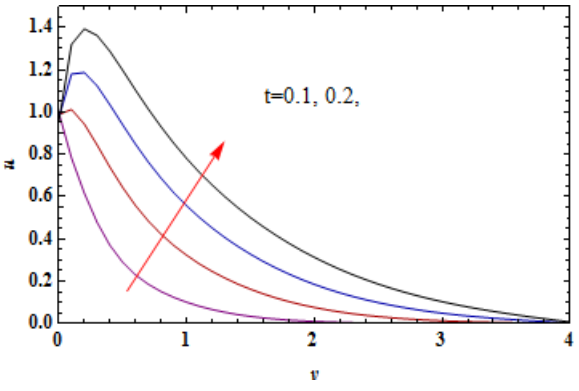

Fig.1 Velocity profile for different values of time t

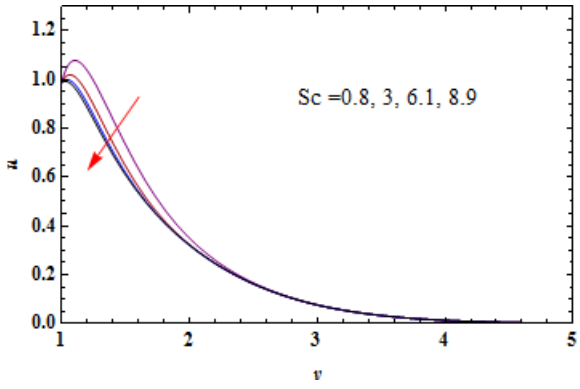

Fig.2 Velocity profile for different values of Sc

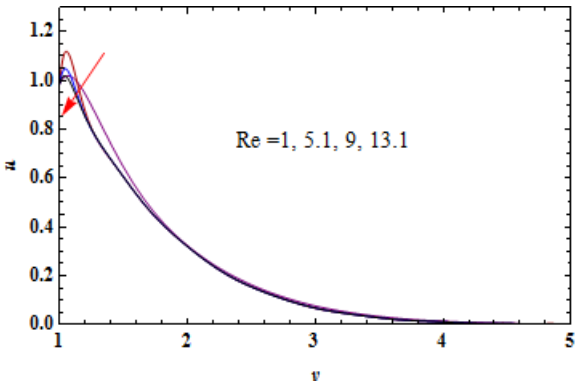

Fig.3 Velocity profile for different values of Re

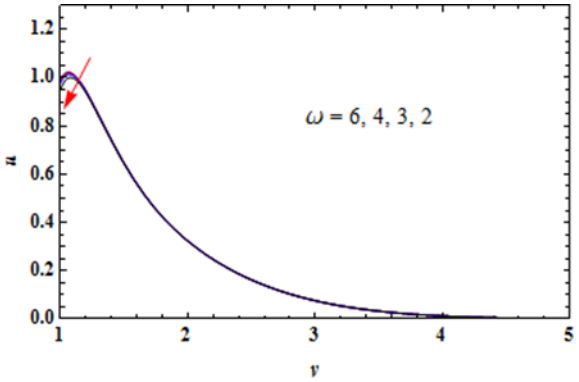

Fig.4 Velocity profile for different values of ω

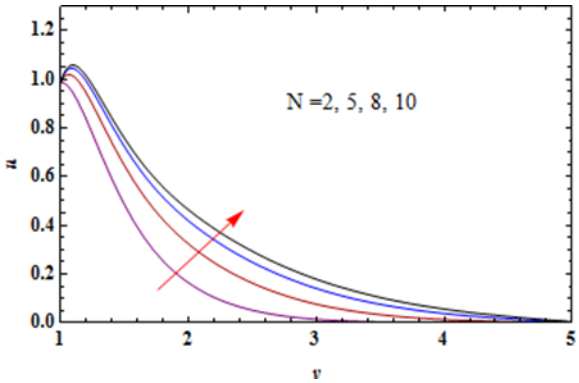

Fig. 5 Velocity profile for different values of N

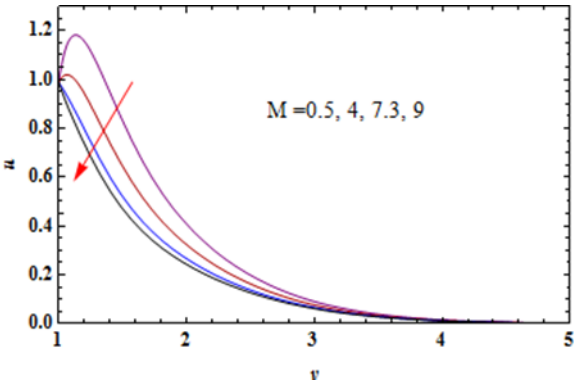

Fig.6 Velocity profile for different values of M

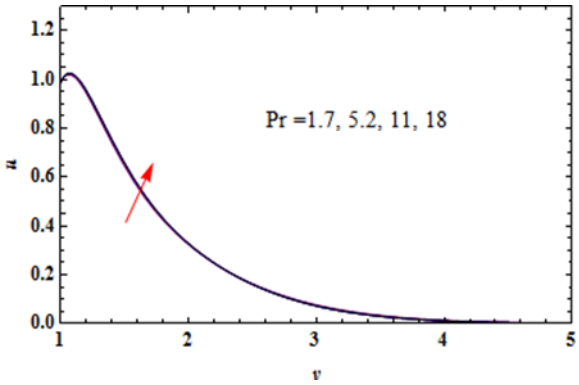

Fig.7 Velocity profile for different values of Pr

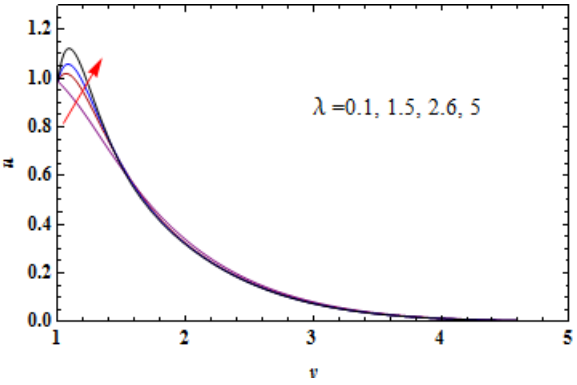

Fig.8 Velocity profile for different values of λ

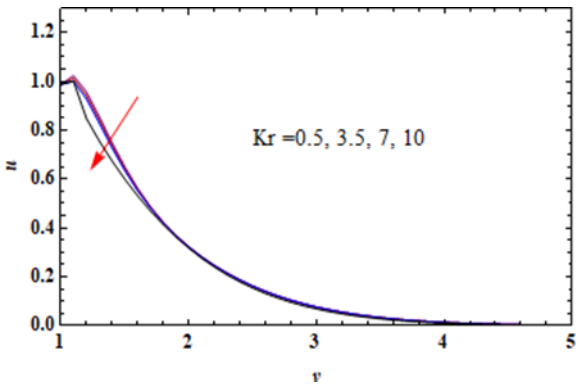

Fig.9 Velocity profile for different values of Kr

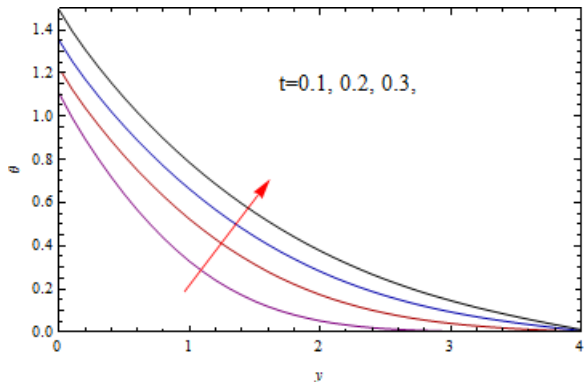

Fig.10 Temperature profile for different values of t

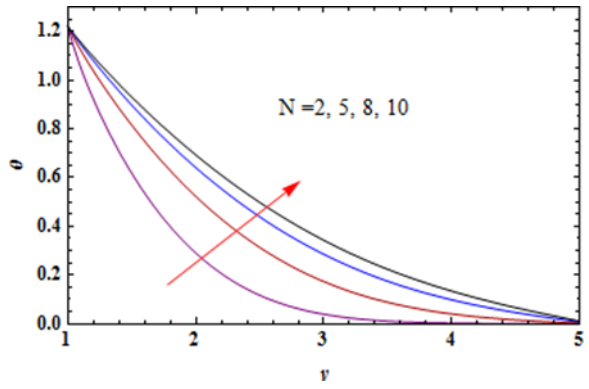

Fig.11 Temperature profile for different values of N

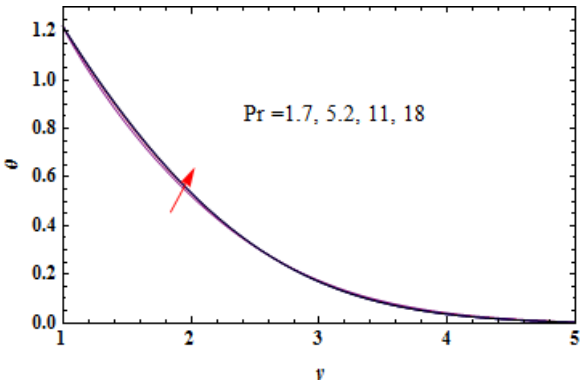

Fig.12 Temperature profile for different values of Pr

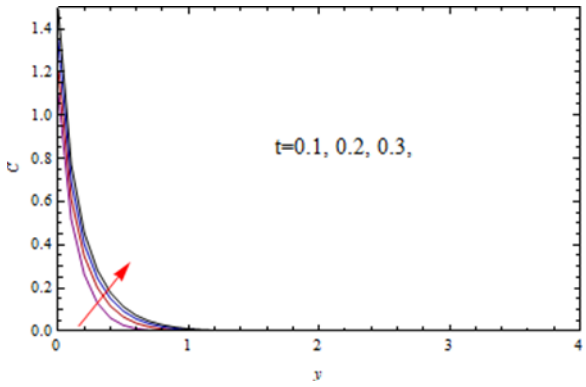

Fig.13 Concentration profile for different values of t

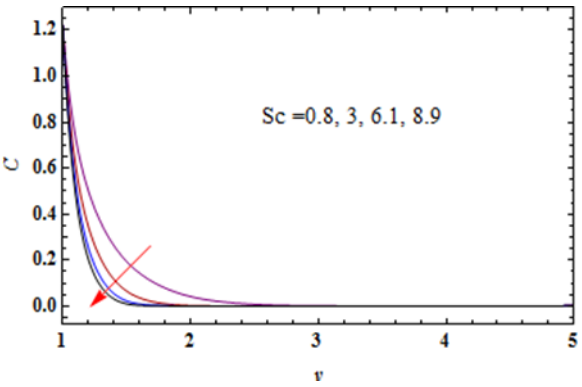

Fig.14 Concentration profile for different values of Sc

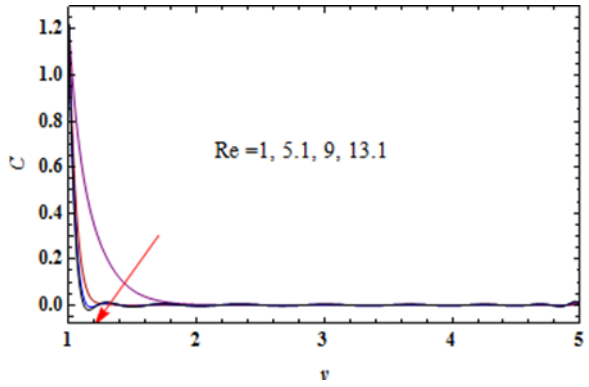

Fig.15 Concentration profile for different values of Re

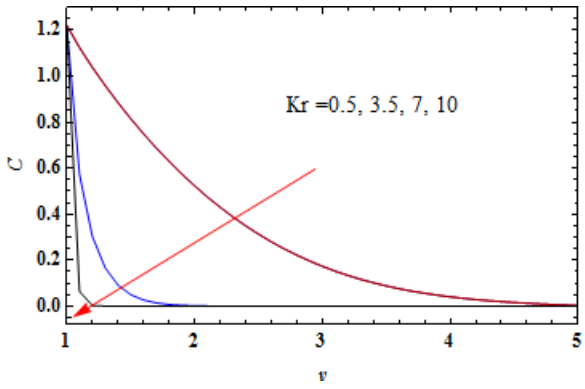

Fig.16 Concentration profile for different values of Kr

Table1- Skin friction coefficient Γ, Nusselt number Nu and Sherwood number Sh for different values of parameters

Re	M	Pr	N	λ	ω	Sc	t	K_r	Γ	Nu	Sh
4	4	1.7	5	1.5	4	3	0.2	2.1	0.102845	0.0747384	0.878289
8.1	4	1.7	5	1.5	4	3	0.2	2.1	0.0219934	0.0740127	1.02994
12	4	1.7	5	1.5	4	3	0.2	2.1	-0.008159	0.0738849	1.07094
18.1	4	1.7	5	1.5	4	3	0.2	2.1	-0.025082	0.0738249	1.0241
8.1	0.5	1.7	5	1.5	4	3	0.2	2.1	0.325529	0.074013	1.02994
8.1	4	1.7	5	1.5	4	3	0.2	2.1	0.0219934	0.074013	1.02994
8.1	7.3	1.7	5	1.5	4	3	0.2	2.1	-0.17184	0.074013	1.02994
8.1	9	1.7	5	1.5	4	3	0.2	2.1	-0.247879	0.074013	1.02994
8.1	4	0.3	5	1.5	4	3	0.2	2.1	0.0210088	0.075103	1.02994
8.1	4	1.7	5	1.5	4	3	0.2	2.1	0.0219934	0.074013	1.02994
8.1	4	4.1	5	1.5	4	3	0.2	2.1	0.0221178	0.073875	1.02994
8.1	4	6.2	5	1.5	4	3	0.2	2.1	0.0221476	0.073842	1.02994
8.1	4	1.7	2	1.5	4	3	0.2	2.1	-0.031508	0.116286	1.02994

8.1	4	1.7	5	1.5	4	3	0.2	2.1	0.0219934	0.740127	1.02994
8.1	4	1.7	8	1.5	4	3	0.2	2.1	0.0420488	0.0586484	1.02994
8.1	4	1.7	10	1.5	4	3	0.2	2.1	0.0501555	0.0525197	1.02994
8.1	4	1.7	5	0.1	4	3	0.2	2.1	0.0274684	0.0740127	1.02994
8.1	4	1.7	5	1.5	4	3	0.2	2.1	0.0219934	0.0740127	1.02994
8.1	4	1.7	5	2.6	4	3	0.2	2.1	0.019402	0.0740127	1.02994
8.1	4	1.7	5	5	4	3	0.2	2.1	0.0164577	0.0740125	1.02994
8.1	4	1.7	5	1.5	6	3	0.2	2.1	0.0159721	0.0740127	1.02994
8.1	4	1.7	5	1.5	4	3	0.2	2.1	0.0219934	0.0740127	1.02994
8.1	4	1.7	5	1.5	3	3	0.2	2.1	0.0303999	0.0740127	1.02994
8.1	4	1.7	5	1.5	2	3	0.2	2.1	0.0542685	0.0740127	1.02994
8.1	4	1.7	5	1.5	4	0.8	0.2	2.1	0.112185	0.0740127	0.890608
8.1	4	1.7	5	1.5	4	3	0.2	2.1	0.0219934	0.0740127	1.02994
8.1	4	1.7	5	1.5	4	6.1	0.2	2.1	-0.0002134	0.0740127	1.06802
8.1	4	1.7	5	1.5	4	8.9	0.2	2.1	-0.0074323	0.0740127	1.08072
8.1	4	1.7	5	1.5	4	3	0.1	2.1	-4.44277	0.963386	10.5829
8.1	4	1.7	5	1.5	4	3	0.2	2.1	0.241928	0.81414	11.3294
8.1	4	1.7	5	1.5	4	3	0.3	2.1	4.12431	0.789501	12.2377
8.1	4	1.7	5	1.5	4	3	0.4	2.1	7.5623	0.807137	13.3061
8.1	4	1.7	5	1.5	4	3	0.2	0.7	0.0241973	0.0740127	1.02465
8.1	4	1.7	5	1.5	4	3	0.2	2.1	0.0219934	0.0740127	1.02994
8.1	4	1.7	5	1.5	4	3	0.2	5.3	0.0174962	0.740127	1.04042
8.1	4	1.7	5	1.5	4	3	0.2	8.3	0.0138685	0.0740127	1.04853

References

[1] Babu M. J. and Sandeep N. (2016). Effect of nonlinear thermal radiation on non-aligned bio-convective stagnation point flow of a magnetic-nanofluid over a stretching sheet, *Alexandria Engineering Journal*, 55(3), 1931-1939.

[2] Rushi K., Palani S. and Kameswaran P. K. (2016). Unsteady MHD flow over a stretching surface with higher order chemical reaction, *Ain Shams Engineering Journal*, 7(1), 399-408.

[3] Mastroberardino A., Madsen M., Hirschhorn J. and Siddique J. I., (2016). Magnetohydrodynamic boundary layer slip flow and heat transfer of power-law fluid over a flat plate, *Journal of Applied Fluid Mechanics*, 9(1), 11-17.

[4] Idowu A. S. and Falodun B. O., (2019). SoretDufour effects on MHD heat and mass transfer of Walters-B viscoelastic fluid over a semi-infinite vertical plate: spectral relaxation analysis, *Journal of taibah university for science*, 13(1), 4962.

[5] Saritha K., Rajasekhar M. N. and Reddy B. S., Combined effects of Soret and Dufour on MHD flow of a power-law fluid over flat plate in slip flow regime, *Int. J. of Applied Mechanics and Engineering*, 23(3)(2018), 689-705.

[6] Malik M. Y. and Khalil-ur-Rehman, Effects of Second Order Chemical Reaction on MHD Free Convection Dissipative Fluid Flow past an Inclined Porous Surface by way of Heat Generation: A Lie Group Analysis, Inf. Sci. Lett., 5(2)(2016), 35-45. 24 A. K. Shukla and Aneesh Jayswal

[7] Imtiaz M., Nazar H. and Hayat T., (2020). Soret and Dufour effects in the flow of viscous fluid by a curved stretching surface, *Pramana - J. Phys.*, 94, Article number 48.

[8] S. Anuradha and N. Harianand, A study of Dufour and Soret effect on MHD mixed convection stagnation point flow towards a vertical plate in a porous medium, International Journal of Fluids Engineering, 9(1)(2017), 1-8.

[9] Ahmed N., (2019). Heat and mass transfer in MHd Poiseuille flow with porous walls, *Journal of Engineering Physics and Thermophysics*, 92(1), 128-136.

[10] Das U. J., and Dorje S.,(2019). Magnetohydrodynamic boundary layer flow with Soret/Dufour effects in presence of heat source and chemical reaction, International Journal of Applied Engineering Research, 14(2), 485-490.

[11] Hayat T., Bashir G., Waqas M., Alsaedi A., (2016). MHD flow of Jeffrey liquid due to a nonlinear radially stretched sheet in presence of Newtonian heating, *Results in Physics* 6, 817–823.

[12] Eswara Rao M., Sreenadh S., (2017). MHD Boundary Layer Flow of Jeffrey Fluid over a Stretching/Shrinking Sheet through Porous Medium, Global *Journal of Pure and Applied Mathematics* ,13(8), 3985-4001.

[13] Hayat T., Sajjad Saif R., Ellahi R., T. Muhammad, A. Alsaedi, (2018). Simultaneous effects of melting heat and internal heat generation instagnation point flow of Jeffrey fluid towards a nonlinear stretching surface with variable thickness, *International Journal of Thermal Sciences* ,132, 344–354.

[14] M.A. Rana, Y. Ali, M. Shoaib, (2018). Three-dimensional Couette flow of a Jeffrey fluid along periodic injection/suction, *Arabian Journal of Mathematical Sciences* ,7, 229–247.

[15] Imran M.A., Miraj F., Khan I., Tlili I., (2018). MHD fractional Jeffrey's fluid flow in the presence of thermo diffusion, thermal radiation effects with first order chemical reaction and uniform heat flux, *Results in Physics* ,10, 10–17.

[16] T. Hayat, S. Asad, A. Alsaedi, F.E. Alsaad, (2015). Radiative Flow of Jeffrey Fluid Through a Convectively Heated Stretching Cylinder, *Journal of Mechanics*, 31(1), 69-78.

[17] K. Das, N. Acharya, P. Kumar Kundu (2015). Radiative flow of MHD Jeffrey fluid past a stretching sheet with surface slip and melting heat Transfer, *Alexandria Engineering Journal* , 54(4), 815–821.

[18] Bhatti M.M., Ali Abbas M., (2016). Simultaneous effects of slip and MHD on peristaltic blood flow of Jeffrey fluid model through a porous Medium, *Alexandria Engineering Journal*, 55(2), 1017–1023.

[19] S. Sreenadh, K. Komala, A.N.S. Srinivas, (2017). Peristaltic pumping of a power – Law fluid in contact with a Jeffrey fluid in an inclined channel with permeable walls, *Ain Shams Engineering Journal*, 8(4), 605–611.

[20] S. Farooq, M. Awais, M. Naseem, T. Hayat, B. Ahmad, (2017). Magneto hydrodynamic peristalsis of variable viscosity Jeffrey liquid with heat and mass transfer, *Nuclear Engineering and Technology*, 49(7), 1396-1404.

[21] K. Venkateswara Raju, A. Parandhama, M.C. Raju, K. Ramesh Babu, (2018). Unsteady MHD Mixed Convection Flow of Jeffrey Fluid Past a Radiating Inclined Permeable Moving Plate in the Presence of thermophoresis Heat Generation and Chemical Reaction, *Journal of Ultra Scientist of Physical Science*s, 30(1), 51-65.

[22] D. Dastagiri Babu, , S. Venkateswarlu, E. Keshava Reddy, (2020). Multivariate Jeffrey Fluid Flow past a Vertical Plate through Porous Medium, *J. Appl. Comput. Mech.*, 6(3), 605-616

[23] Brice Carnahan, H.A. Luther and James O. Wilkes. (1990). Applied Numerical Methods, Krieger Pub Co, Florida.

[24] R. Siegel and J. R. Howell, Thermal Radiation Heat Transfer, Taylor & Francis, London, (1992).